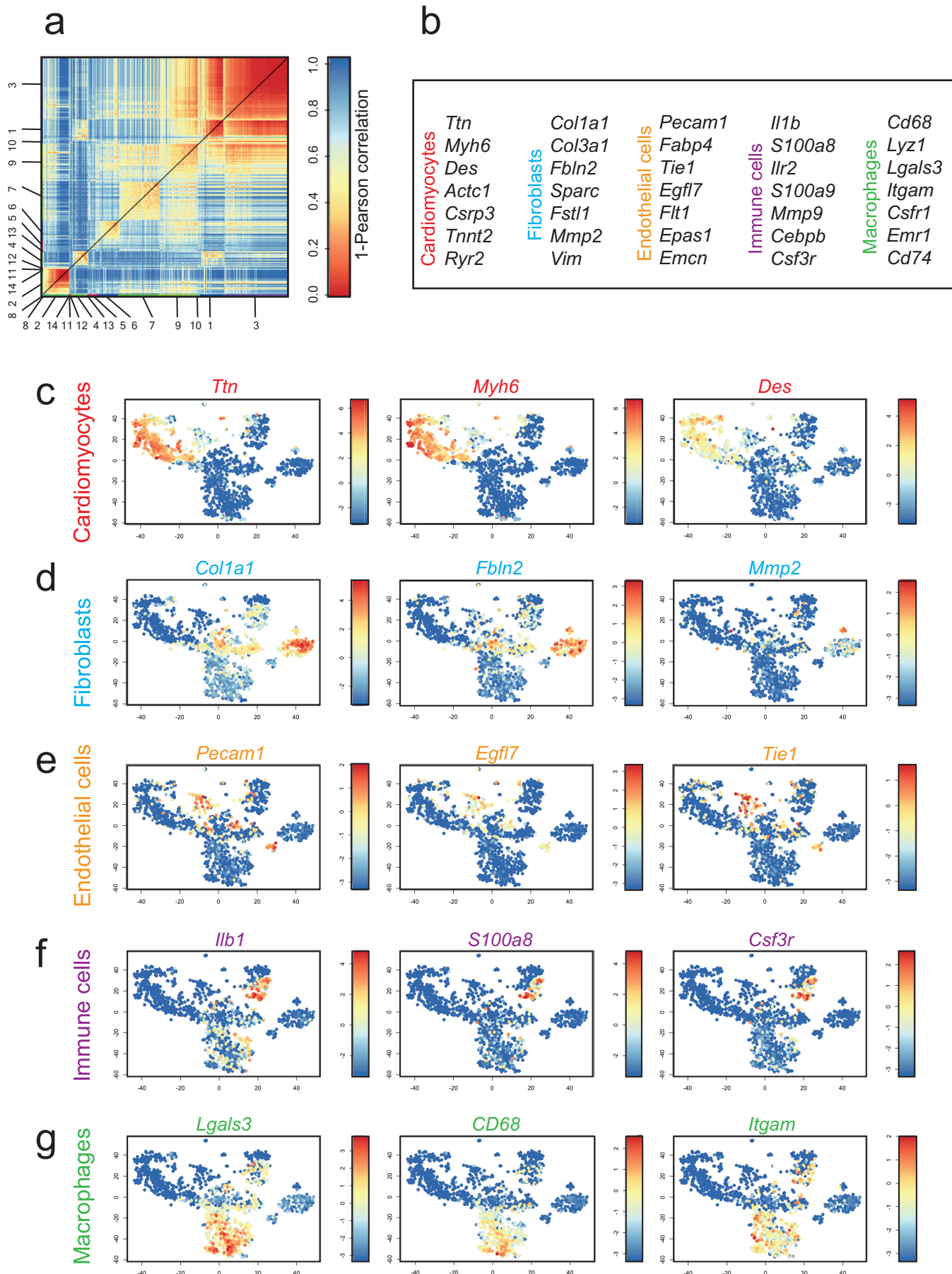


Supplementary information

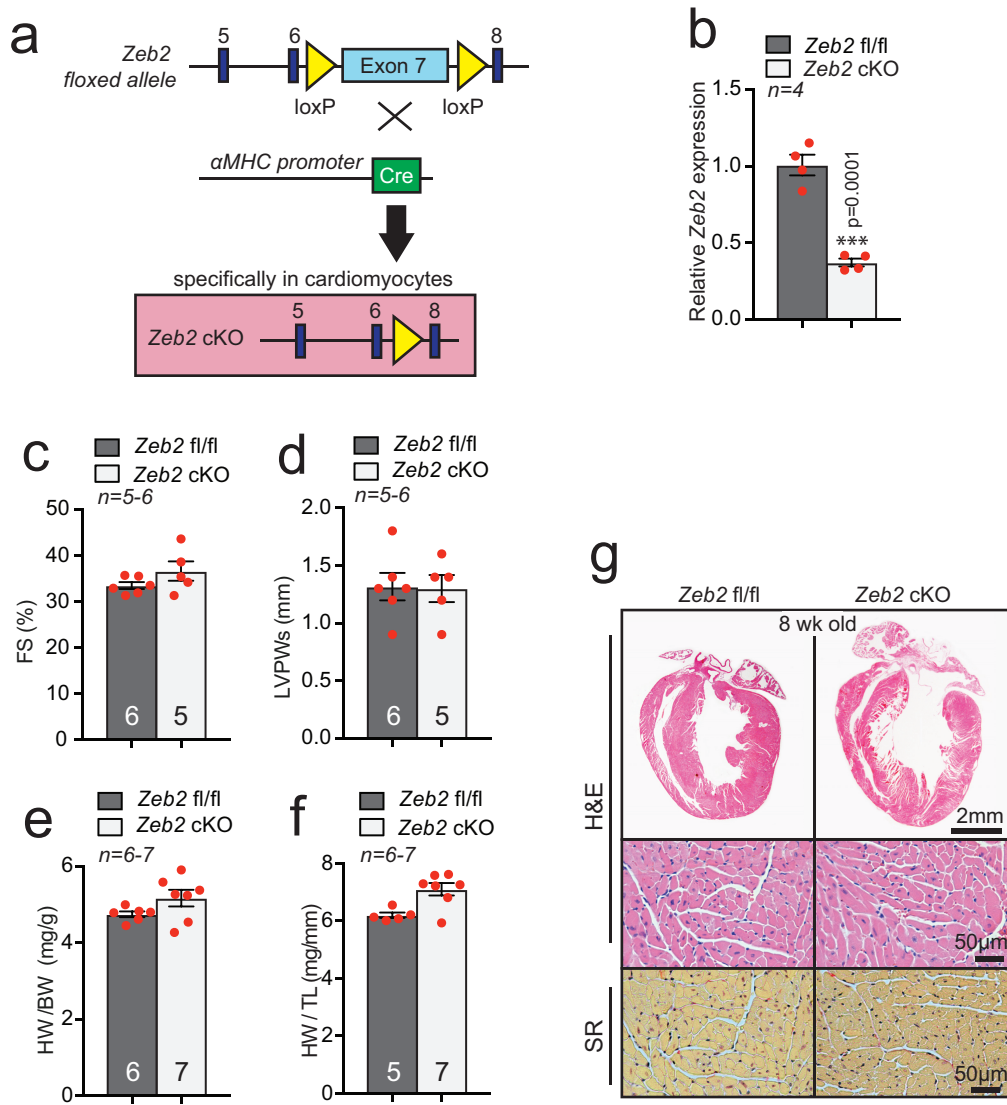
Cardiomyocytes stimulate angiogenesis after ischemic injury in a ZEB2-dependent manner

Authors: Monika M. Gladka¹, Arwa Kohela¹, Bas Molenaar¹, Danielle Versteeg^{1,2}, Lieneke Kooijman¹, Jantine Monshouwer-Kloots¹, Veerle Kremer^{3,4}, Harmjan R. Vos⁵, Manon M.H. Huibers⁶, Jody J. Haigh⁷, Danny Huylebroeck^{8,9}, Reinier A. Boon^{3,10,11} Mauro Giacca¹², Eva van Rooij^{1,2*}



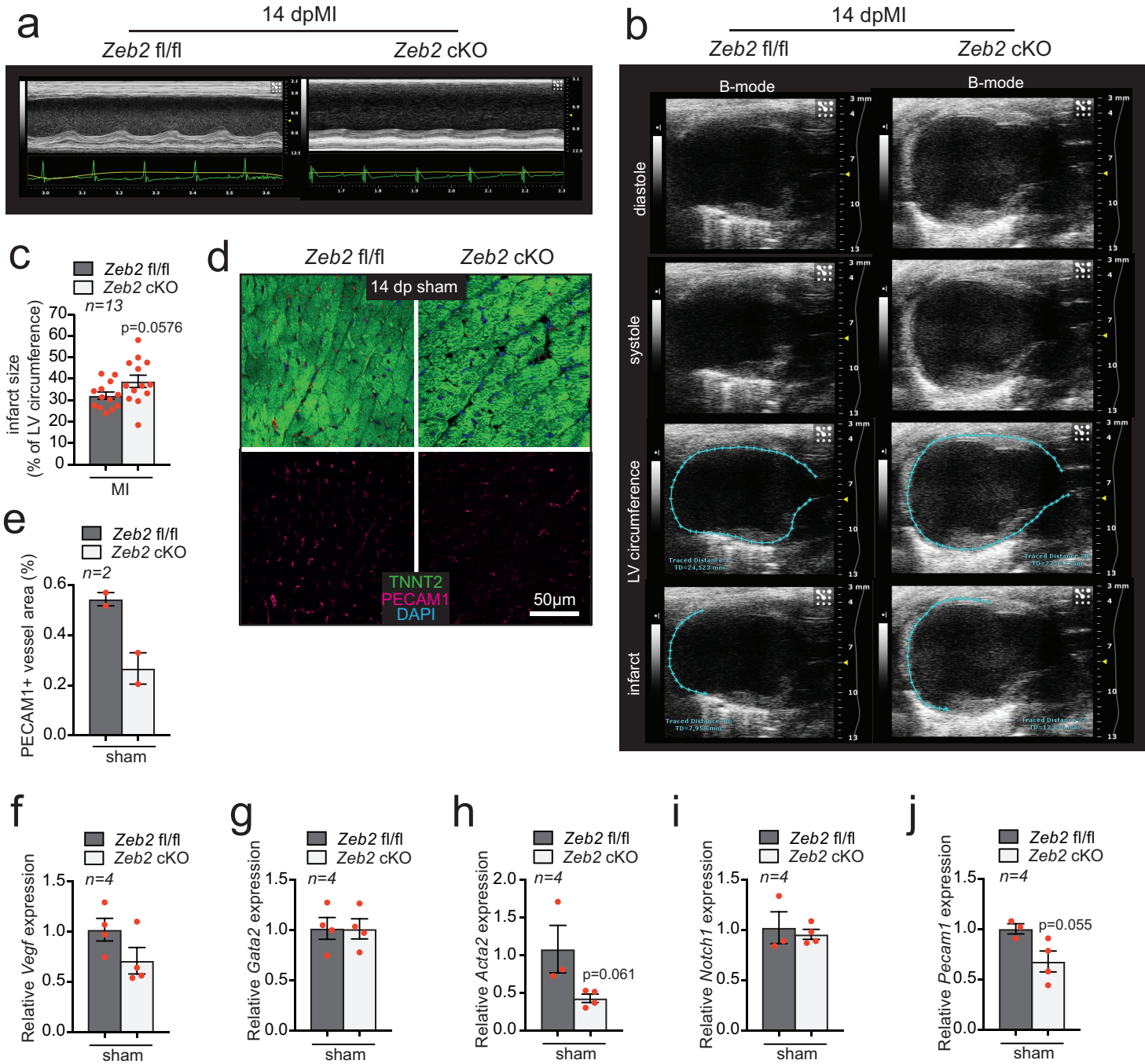
Supplementary Figure 1. Clustering of cardiac cells based on gene expression differences. **a** Heatmap showing distances in cell-to-cell transcriptomes of cells obtained from sham and 3 dpMI hearts. Distances are measured by 1-Pearson's correlation coefficient.

K-medoids clustering identified 14 different cell clusters depicted on the x and y axes of the heatmap. **b** Table showing a list of known marker genes of main cardiac cell types used to identify the subpopulations of cells identified in **Fig. 1c**. **c-g** t-SNE maps indicating the expression of selected, well-established cellular markers in cell populations identified as **c** cardiomyocytes, **d** fibroblasts, **e** endothelial cells, **f** Immune cells, **g** macrophages. Data are shown as normalized transcript counts on a color-coded logarithmic scale. T-SNE indicates t-distributed stochastic neighbor embedding.

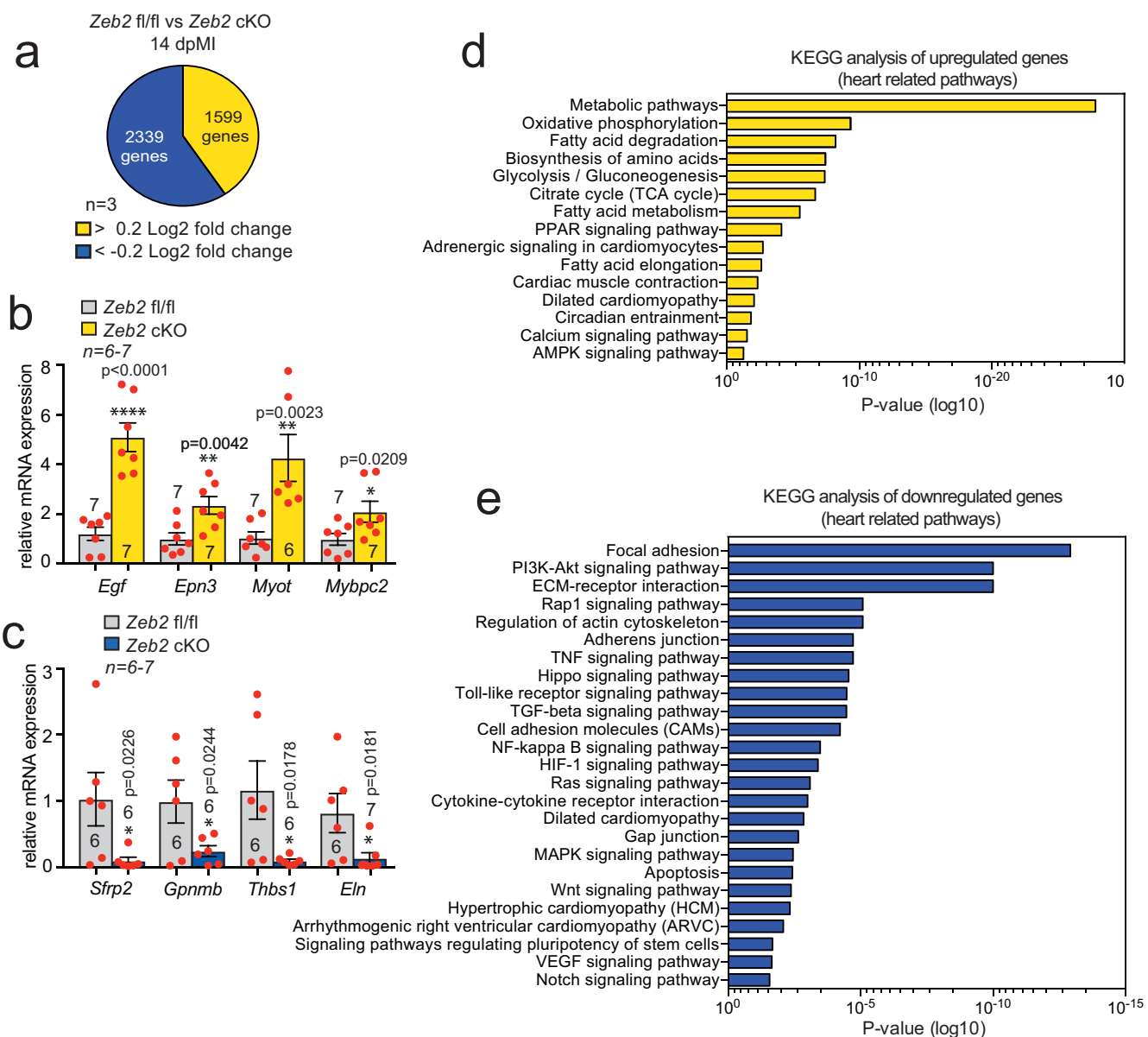


Supplementary Figure 2. Generation of a cardiomyocyte-specific Zeb2 cKO mouse model.

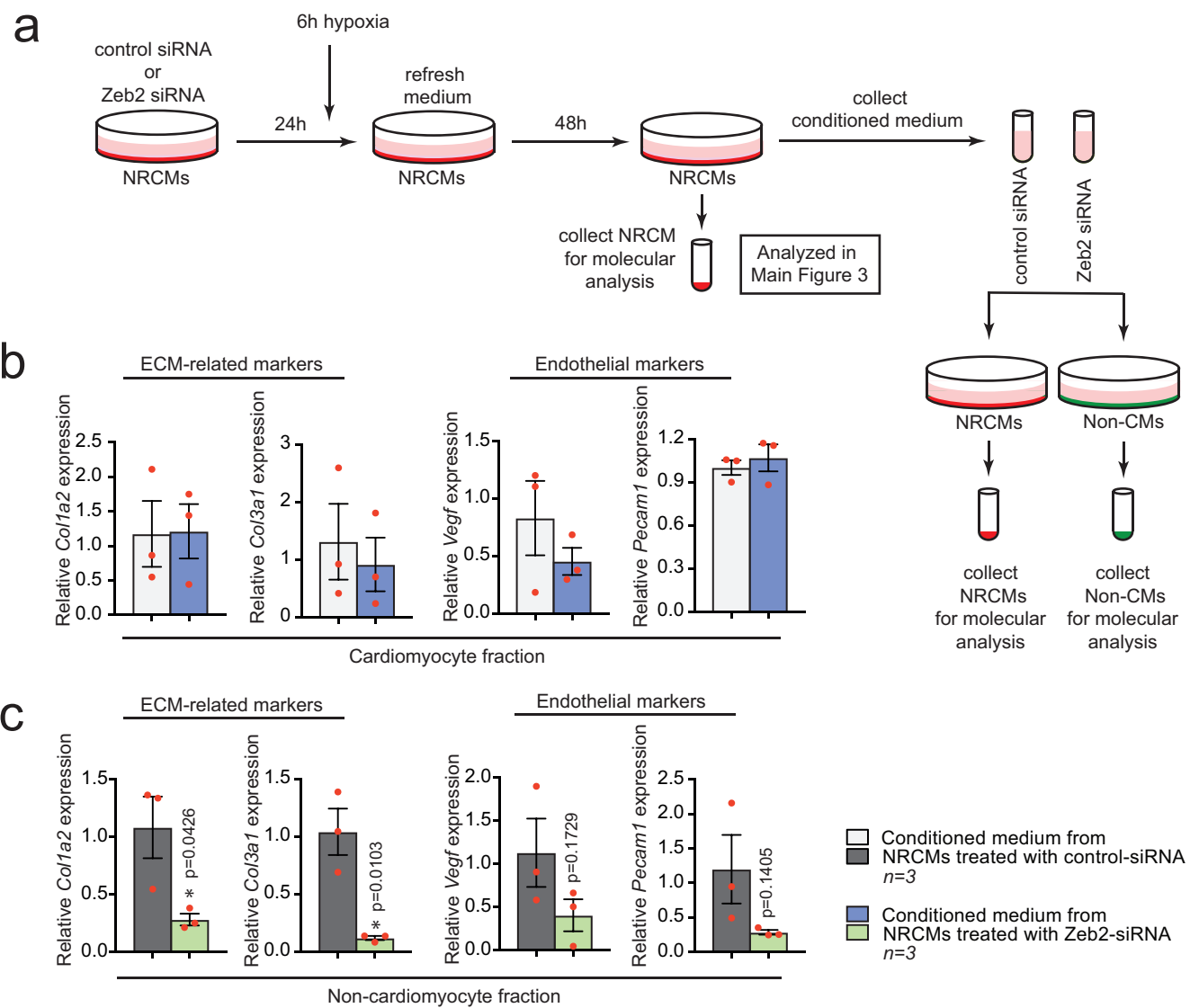
a Schematic representation of generation of the Zeb2 cardiac KO (cKO). **b** mRNA expression level of Zeb2 in hearts from Zeb2 fl/fl and Zeb2 cKO mice. **c-d** Quantification of **c** fractional shortening (FS) and **d** left ventricular internal diameter in systole (LVIDs) from adult Zeb2 fl/fl and Zeb2 cKO mice. **e-f** Quantification of **e** HW/BW and **f** HW/TL ratio in Zeb2 fl/fl and Zeb2 cKO mice. **g** Representative images of four-chamber view (top panel), H&E stained sections (second panel) and SR stained sections (third panel) of hearts collected from adult Zeb2 fl/fl and Zeb2 cKO mice. H&E indicates Hematoxylin and Eosin, SR indicates Sirius Red, HW/BW indicates heart weight to body weight ratio, HW/TL indicates heart weight to tibia length ratio. Data are represented as mean \pm SEM, ***p<0.0001 each dot indicates a biological replicate, n is indicated in figures. Comparison of two groups was performed with the unpaired, two-tailed Student's t-test between Zeb2 cKO vs Zeb2 fl/fl (**b, c, d, e, f**) Source data are provided as a Source Data file.



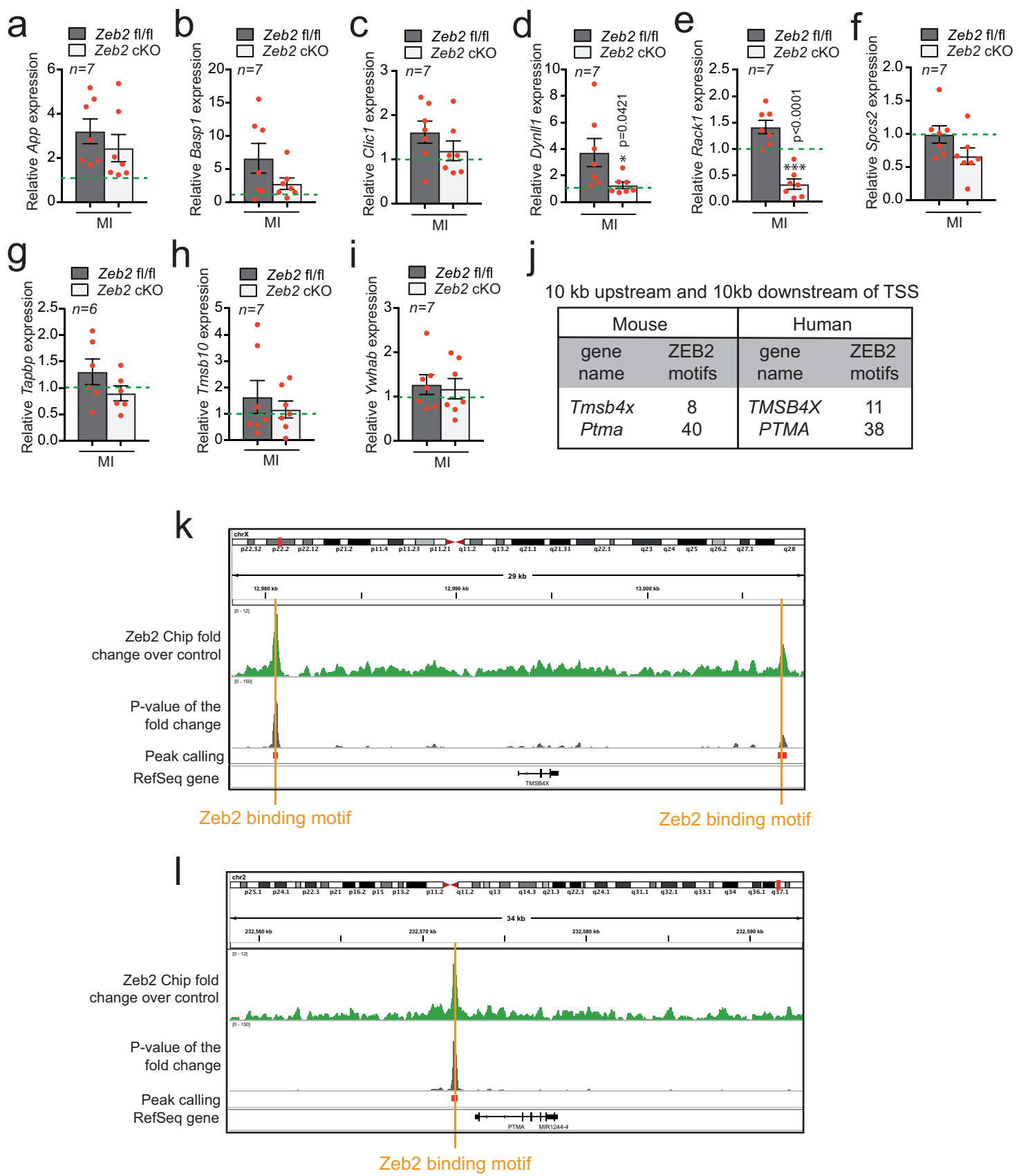
Supplementary Figure 3. Cardiomyocytes-specific ZEB2 deletion impairs cardiac function after injury. **a** Echocardiographic images of m-mode in hearts from Zeb2 fl/fl and Zeb2 cKO mice subjected to MI for 14 days. **b** Representative b-mode images of long access view in diastole and systole indicating infarcted region by measurements of percentage of LV circumference and **c** its quantification. **d** Immunofluorescence for PECAM1, TNNT2 and DAPI in Zeb2 fl/fl and Zeb2 cKO sham hearts **e** quantification of PECAM1 positive blood vessel area in histological sections from **(d)**. Data in **d-e** from n=2. **f-j** mRNA expression levels of **f** Vegf and **g** Gata2 **h** Acta2 **i** Notch1 **j** Pecam1 in Zeb2 fl/fl and Zeb2 cKO sham mice. Data are represented as mean \pm SEM, each dot indicates a biological replicate, n is indicated in figures. Comparison of two groups was performed with the unpaired, two-tailed Student's t-test between Zeb2 cKO vs Zeb2 fl/fl post-MI (**c**) or post-sham (**f, g, h, i, j**). Source data are provided as a Source Data file.



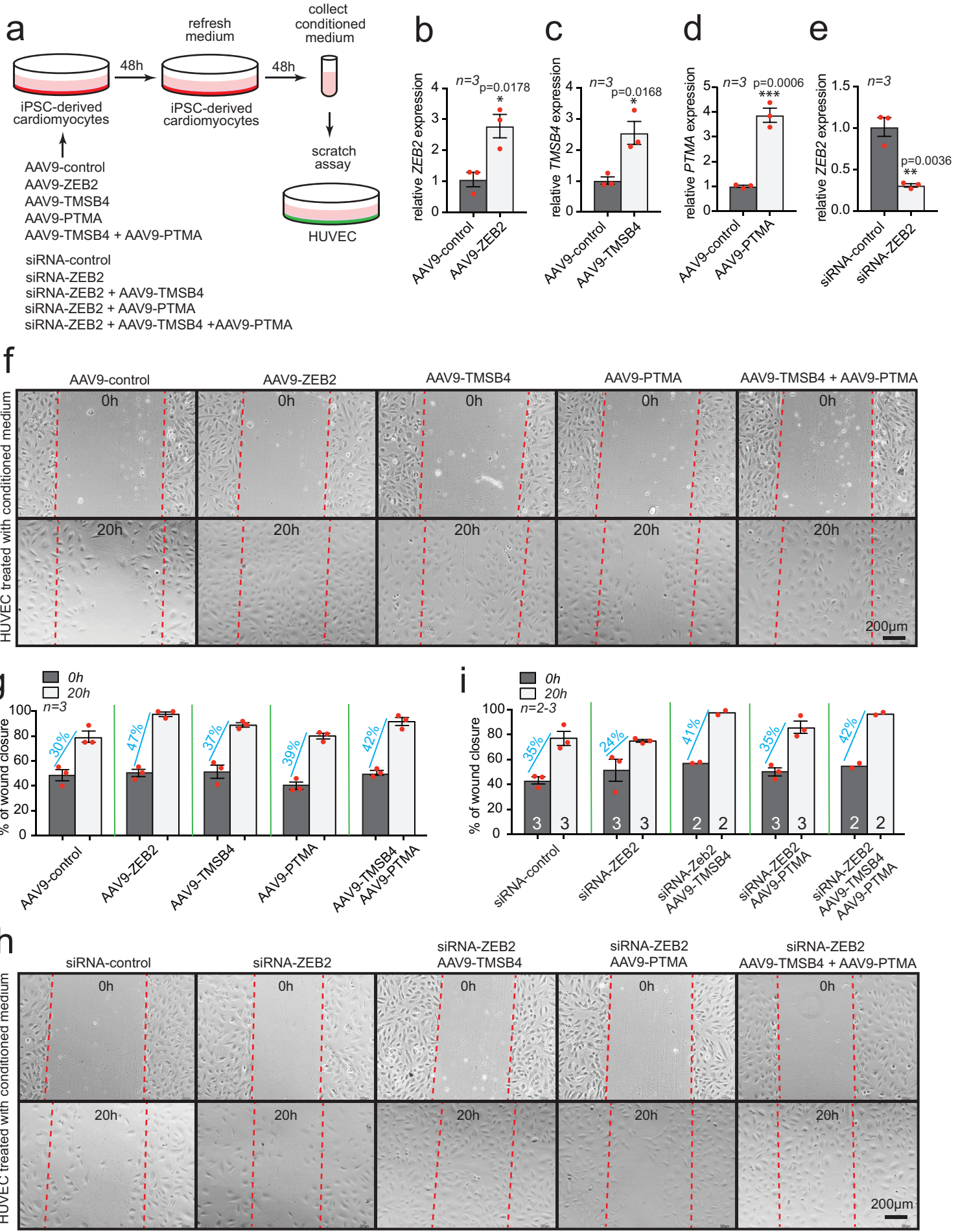
Supplementary Figure 4. RNA-seq to identify the role of ZEB2 in the injured heart. **a** Representation of the RNA-seq dataset as pie diagram showing down- and upregulated genes in Zeb2 fl/fl and Zeb2 cKO heart tissue 14 dpMI. **b-c** mRNA expression levels of **b** upregulated and **c** downregulated genes. **d-e** KEGG pathway analysis on genes significantly **d** upregulated and **e** downregulated in Zeb2 cKO hearts when compared to Zeb2 fl/fl hearts post injury. Data are represented as mean \pm SEM, * $p<0.05$, ** $p<0.01$, **** $p<0.0001$, each dot indicates a biological replicate, n is indicated in figures. Comparison of two groups was performed with the unpaired, two-tailed Student's t-test between Zeb2 cKO vs Zeb2 fl/fl post-MI (**b, c**). Source data are provided as a Source Data file.



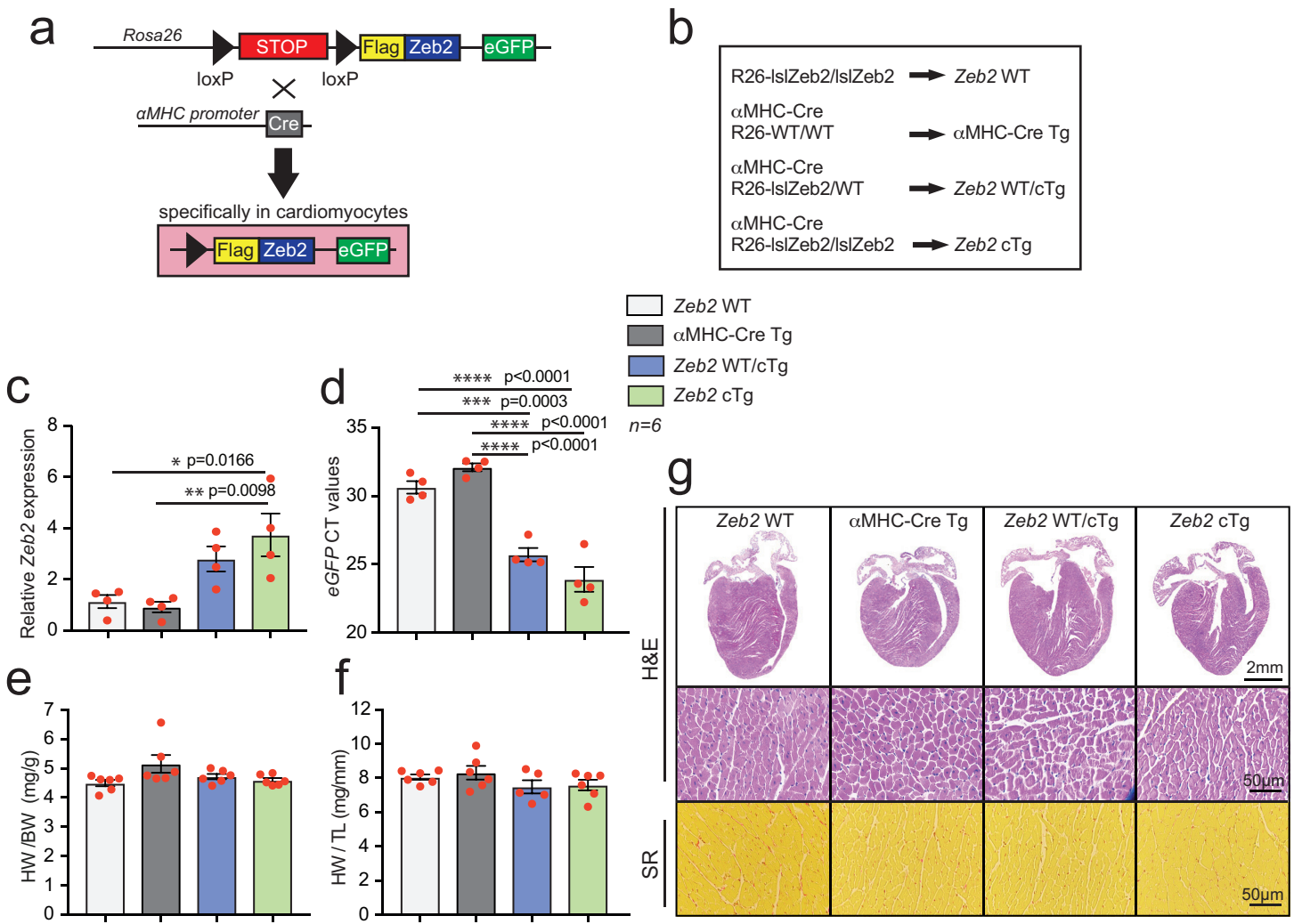
Supplementary Figure 5. Cellular communication is ZEB2 dependent. **a** Experimental setup to produce and collect conditioned medium from NRCMs treated with ZEB2 silencing RNA. **b-c** mRNA expression levels of fibroblast and endothelial markers in **b** NRCMs **c** non-cardiomyocytes treated with conditioned media collected in **(a)**. Data are represented as mean \pm SEM, * $p<0.05$, each dot indicates a biological replicate, n is indicated in figures. Comparison of two groups was performed with the unpaired, two-tailed Student's t-test (**b, c**). Source data are provided as a Source Data file.



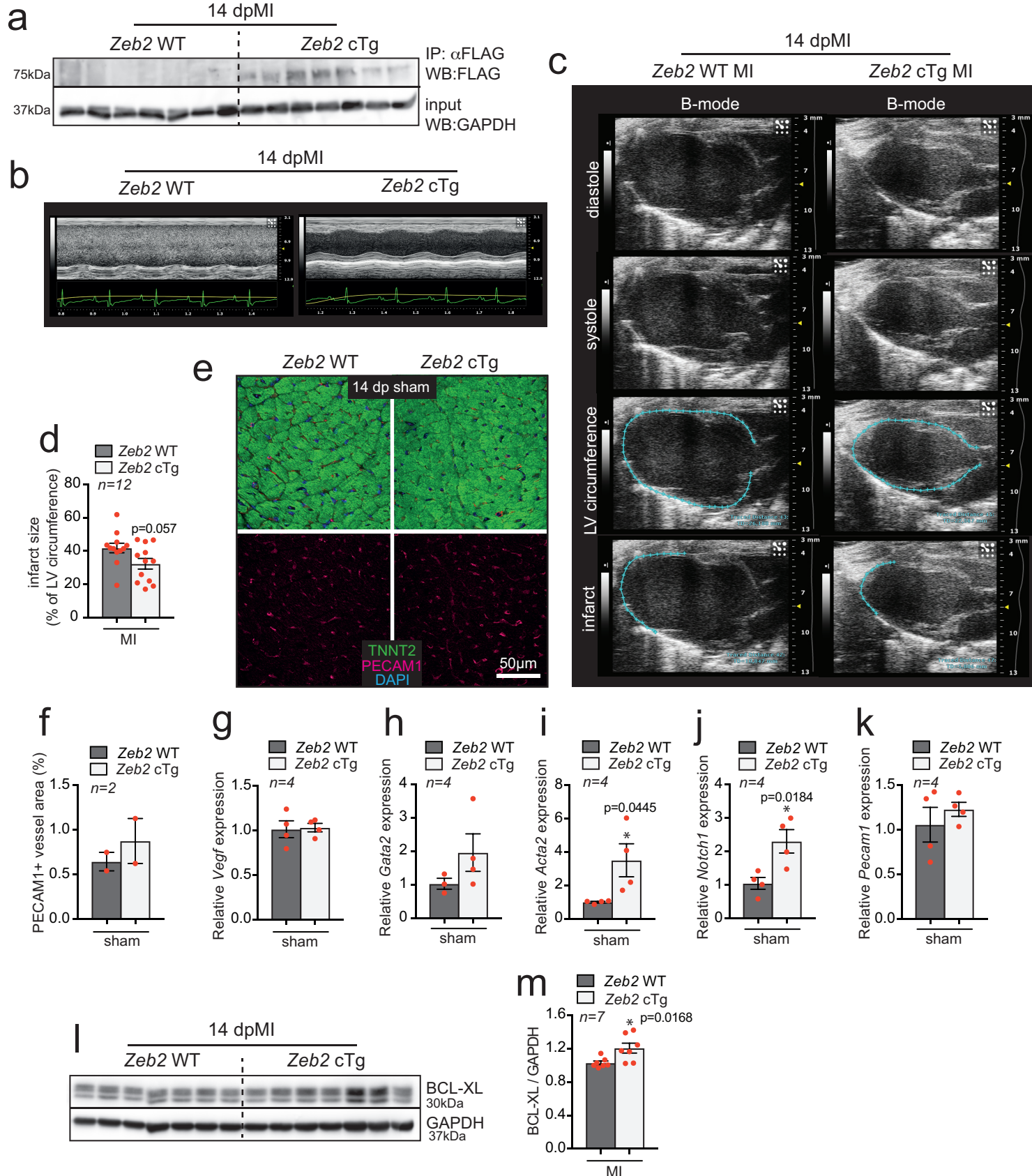
Supplementary Figure 6. Validation of factors identified by mass spectrometry *in vivo*. **a-i** mRNA expression levels of **a** App, **b** Basp1, **c** Clic1, **d** Dynll1, **e** Rack1, **f** Spcs2, **g** Tapbp, **h** Tmsb10, **i** Ywhab in hearts from Zeb2 fl/fl and Zeb2 cKO mice. **j** ZEB2 predicted binding sites in 10kb upstream and 10kb downstream region of the transcription starting site (TSS) of Tmsb4 and Ptma in mouse and human. **k-l** ZEB2 protein directly binds to **k** TMSB4 and **l** PTMA promoters. Green dashed line indicates sham Zeb2 fl/fl control. Orange line denotes ZEB2 binding motifs. Data are represented as mean \pm SEM, * $p<0.05$, *** $p<0.001$, each dot indicates a biological replicate, n is indicated in figures. Comparison of two groups was performed with the unpaired, two-tailed Student's t-test between Zeb2 cKO vs Zeb2 fl/fl groups post-MI (**a, b, c, d, e, f, g, h, i**). Source data are provided as a Source Data file.



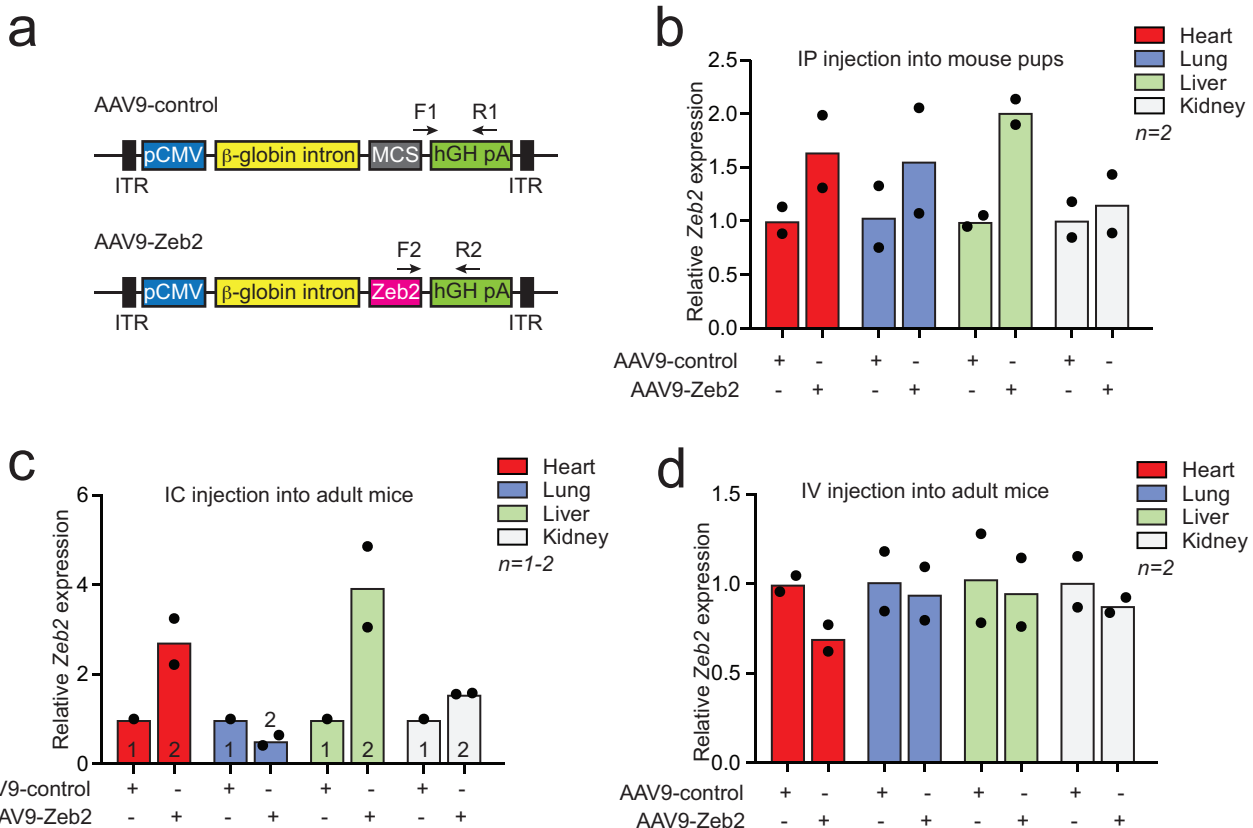
Supplementary Figure 7. Expression of ZEB2, TMSB4 and PTMA in cardiomyocytes drives endothelial cell migration. **a** Conditioned medium experimental setup. **b-e** mRNA expression levels of **(b)**, **e** ZEB2, **c** TMSB4 **d** PTMA in iPSC-derived cardiomyocytes treated with AAV9-control, AAV9-ZEB2, AAV9-TMSB4, AAV9-PTMA or siRNA-control and siRNA ZEB2, respectively **f** Representative images of scratch assay in HUVECs treated with indicated conditioned medium at 0 and 20 hours after treatment. **g** Quantification of wound closure from **(f)**. **h** Representative images of scratch assay in HUVECs treated with the indicated conditioned media at 0 and 20 hours after treatment. **i** Quantification of wound closure from **(h)**. Data in **f-h** is from one experiment with 2-3 biological replicates. Data are represented as mean \pm SEM, * $p<0.05$, *** $p<0.001$, each dot indicates a biological replicate, n is indicated in figures. Comparison of two groups was performed with the unpaired, two-tailed Student's t-test (**b, c, d, e**). Source data are provided as a Source Data file.



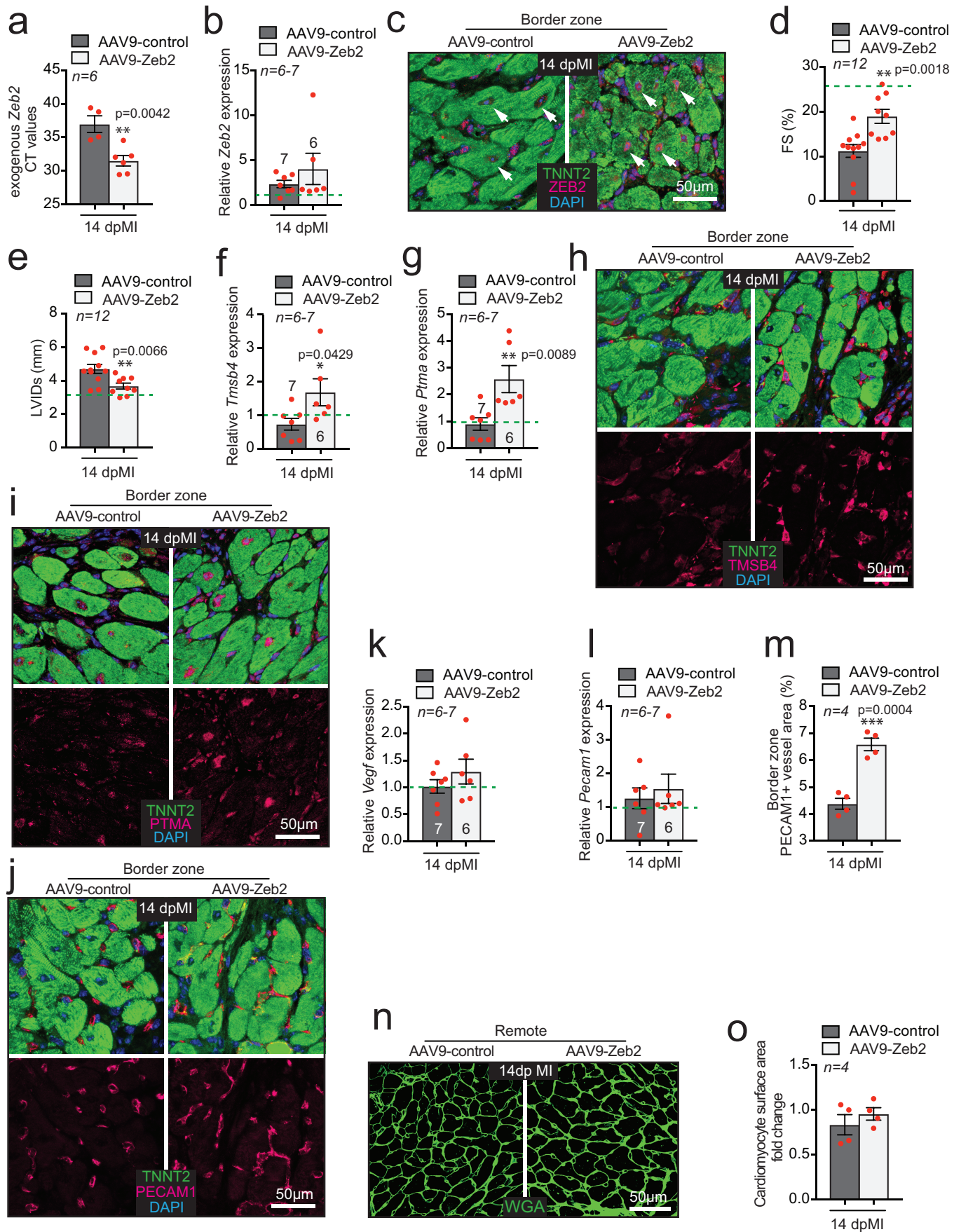
Supplementary Figure 8. Generation of a cardiomyocyte-specific Zeb2 cTg mouse model. **a** Schematic representation of generation of the ZEB2 cardiac overexpression model (Zeb2 cTg). **b** Detailed description of the used genotypes and their simplified names. **c-d** mRNA expression levels of **c** Zeb2 and **d** eGFP (CT values) in hearts from Zeb2 WT and Zeb2 cTg mice. **e-f** Quantification of **e** HW/BW and **f** HW/TL ratio in Zeb2 WT and Zeb2 cTg mice. **g** Representative images of four-chamber view (top panel), H&E stained sections (second panel) and SR stained sections (third panel) of hearts collected from adult Zeb2 WT and Zeb2 cTg mice. H&E indicates Hematoxylin and Eosin, SR indicates Sirius Red, HW/BW indicates heart weight to body weight ratio, HW/TL indicates heart weight to tibia length ratio. Data are represented as mean \pm SEM, *p<0.05, **p<0.01, ***p<0.001, ****p<0.0001, each dot indicates a biological replicate, n is indicated in figures. Data were analysed by ordinary one-way ANOVA with Tukey multiple comparison test (**c**, **d**, **e**, **f**). Source data are provided as a Source Data file.



Supplementary Figure 9. Cardiomyocyte-specific ZEB2 overexpression protects cardiac function after MI. **a** FLAG immunoprecipitation in heart tissue from Zeb2 WT and Zeb2 cTg 14 dpMI. **b** Echocardiographic images of m-mode in hearts from Zeb2 WT and Zeb2 cTg mice subjected to MI for 14 days. **c** Representative b-mode images of long access view in diastole and systole indicating infarcted region by measurements of percentage of LV circumference and **d** its quantification. **e** Immunofluorescence for PECAM1, TNNT2 and DAPI in Zeb2 WT and Zeb2 cTg sham hearts **f** quantification of PECAM1 positive blood vessel area in histological sections from (**e**). Data in **e-f** from n=2. **g-k** mRNA expression levels of **g** Vegf and **h** Gata2 **i** Acta2 **j** Notch1 **k** Pecam1 in Zeb2 WT and Zeb2 cTg sham mice. **l** Representative WB for BCL-XL in tissue from Zeb2 WT and Zeb2 cTg 14 dpMI and **m** its quantification. Data are represented as mean \pm SEM, *p<0.05, each dot indicates a biological replicate, n is indicated in figures. Comparison of two groups was performed with the unpaired, two-tailed Student's t-test between Zeb2cTg vs Zeb2 WT post-MI (**d, m**) or post-sham (**f, g, h, i, j, k**). Source data are provided as a Source Data file.



Supplementary Figure 10. Efficiency of AAV9-Zeb2 delivery in vivo. **a** Schematic representation of constructs used to generate AAV9 viruses. **b-d** mRNA expression level of Zeb2 in the indicated organs of **b** intraperitoneal (IP), **c** intracardiac (IC) and **d** intravenous (IV) AAV9-Zeb2-injected mice. Data are represented as mean \pm SEM, each dot indicates a biological replicate, n is indicated in figures. Source data are provided as a Source Data file.



Supplementary Figure 11. AAV9-mediated ZEB2 delivery is cardioprotective. **a-b** Expression levels of **a** exogenous Zeb2 and **b** Zeb2 mRNA in AAV9-control and AAV9-Zeb2 treated mice 14 days post-surgery. **c** Immunohistochemistry for ZEB2, TNNT2 and DAPI nuclei of histological sections of hearts from AAV9-control and AAV9-Zeb2 treated mice 14 dpMI (border zone). **d-e** Quantification of **d** fractional shortening (FS) and **e** left ventricular internal diameter in systole (LVIDs) from AAV9-control and AAV9-Zeb2 treated mice 14 dpMI. **f-g** mRNA expression levels of **f** Tmsb4 and **g** Ptma in hearts from AAV9-control and AAV9-Zeb2 treated mice 14 days post-MI. **h-i** Immunofluorescence for **h** TMSB4 or **i** PTMA, ACTN2 and DAPI nuclei of histological sections of hearts from AAV9-control and AAV9-Zeb2 treated mice 14 dpMI. **j** Immunofluorescence for PECAM1, TNNT2 and DAPI nuclei of histological sections of hearts from AAV9-control and AAV9-Zeb2 treated mice 14 dpMI. **k-l** mRNA expression level of **k** Vegf and **l** Pecam1 in hearts from AAV9-control and AAV9-Zeb2 treated mice 14 dpMI. **m** Quantification of PECAM1 positive blood vessel area in histological sections of hearts from AAV9-control and AAV9-Zeb2 treated mice 14 dpMI. **n** WGA staining to measure cardiomyocyte surface area and **o** its quantification. Green dashed line indicates sham AAV9-control. White arrows show ZEB2 positive cardiomyocytes. Data are represented as mean \pm SEM, * $p<0.05$, ** $p<0.01$, *** $p<0.001$, each dot indicates a biological replicate, n is indicated in figures. Comparison of two groups was performed with the unpaired, two-tailed Student's t-test between AAV9-Zeb2 vs AAV9-control post-MI (**a, b, d, e, f, g, k, l, m, o**). Source data are provided as a Source Data file.

Supplementary Table 1. Morphometric and echocardiographic characteristic of Zeb2 fl/fl and Zeb2 cKO mice.

	Zeb2 fl/fl	Zeb2 cKO
n	6	6
BW (g)	20,8 ± 1,99	21,7 ± 2,28
HW (g)	0,10 ± 0,01	0,11 ± 0,01
TL (mm)	15,3 ± 0,53	15,7 ± 0,55
IVSd (mm)	0,86 ± 0,13	0,94 ± 0,24
IVSs (mm)	1,33 ± 0,12	1,42 ± 0,2
LVIDd (mm)	3,83 ± 0,13	3,94 ± 0,23
LVIDs (mm)	2,56 ± 0,16	2,6 ± 0,25
LVPWd (mm)	0,93 ± 0,17	0,9 ± 0,25
LVPWs (mm)	1,31 ± 0,29	1,3 ± 0,26
EF (%)	62,8 ± 2,6	66,5 ± 5,4
FS (%)	33,4 ± 1,8	36,6 ± 4,6
Heart rate	435 ± 24	436 ± 25

BW, body weight; HW, heart weight; TL, tibia length; IVSd, interventricular septal thickness at end-diastole; IVSs, interventricular septal thickness at end-systole; LVIDd, left ventricular internal dimension at end-diastole; LVIDs, left ventricular internal dimension at end-systole; LVPWd, left ventricular posterior wall thickness at end-diastole; LVPWs, left ventricular posterior wall thickness at end-systole; EF, ejection fraction; FS, fractional shortening; Data are expressed as means ± STDEV. Comparison of two groups was performed with the unpaired, two-tailed Student's t-test between Zeb2 cKO vs Zeb2 fl/fl.

Supplementary Table 2. Morphometric and echocardiographic characteristic of Zeb2 fl/fl and Zeb2 cKO mice subjected to sham or MI for 14 days.

	Zeb2 fl/fl	Zeb2 cKO
Surgery	sham	sham
n	6	7
BW (g)	26,1 ± 2,47	28 ± 1,22
HW (g)	0,13 ± 0,01	0,13 ± 0,01
TL (mm)	16,3 ± 0,63	16,7 ± 0,35
IVSd (mm)	1,71 ± 0,55	1,33 ± 0,35
IVSs (mm)	2,17 ± 0,49	1,79 ± 0,42
LVIDd (mm)	3,78 ± 0,52	4,08 ± 0,54
LVIDs (mm)	2,58 ± 0,62	2,9 ± 0,71
LVPWd (mm)	1,22 ± 0,28	1,1 ± 0,13
LVPWs (mm)	1,74 ± 0,35	1,39 ± 0,29
EF (%)	61,6 ± 10,3	59,9 ± 11,6
FS (%)	33,1 ± 7,3	32,1 ± 7,9
Heart rate	411 ± 44	407 ± 29
	Zeb2 fl/fl	Zeb2 cKO
Surgery	MI	MI
n	10	11
BW (g)	28,9 ± 1,65	28,4 ± 2,84
HW (g)	0,17 ± 0,02	0,19 ± 0,04
TL (mm)	16,7 ± 0,53	16,4 ± 0,54
IVSd (mm)	1,26 ± 0,44	1,05 ± 0,27
IVSs (mm)	1,60 ± 0,63	1,23 ± 0,35
LVIDd (mm)	5,10 ± 0,89 \$\$ p=0.0094	5,41 ± 0,65
LVIDs (mm)	4,05 ± 1,09 \$ p=0.0227	4,62 ± 0,84
LVPWd (mm)	1,31 ± 0,44	1,15 ± 0,47
LVPWs (mm)	1,54 ± 0,39	1,37 ± 0,57
EF (%)	44,7 ± 13,6	32,7 ± 14,5 # p=0.0450
FS (%)	23,5 ± 8,4 \$ p=0.0382	16,1 ± 7,6 # p=0.0238
Heart rate	415 ± 42	424 ± 28

sham, sham-operated control group; MI, myocardial infarction; BW, body weight; HW, heart weight; TL, tibia length; IVSd, interventricular septal thickness at end-diastole; IVSs, interventricular septal thickness at end-systole; LVIDd, left ventricular internal dimension at end-diastole; LVIDs, left ventricular internal dimension at end-systole; LVPWd, left ventricular posterior wall thickness at end-diastole; LVPWs, left ventricular posterior wall thickness at end-systole; EF, ejection fraction; FS, fractional shortening; Data are expressed as means ± STDEV. Comparison of two groups was performed with the unpaired, two-tailed Student's t-test between Zeb2 fl/fl post-MI vs Zeb2 fl/fl post-sham (indicated by dollar sign, \$p<0.05, \$\$p<0.01) and Zeb2 cKO post-MI vs Zeb2 fl/fl post-MI (indicated by pound sign, #p<0.05).

Supplementary Table 3. Morphometric and echocardiographic characteristic of Zeb2 WT, α MHC-Cre Tg, Zeb2 WT/cTg and Zeb2 cTg mice.

	Zeb2 WT	aMHC-Cre Tg	Zeb2 WT/cTg	Zeb2 cTg
n	6	6	6	6
BW (g)	31,4 ± 1,46	28,48 ± 1,36	28,45 ± 2,5	28,71 ± 2,47
HW (g)	0,14 ± 0,01	0,15 ± 0,02	0,13 ± 0,01	0,13 ± 0,01
TL (mm)	17,51 ± 0,37	17,61 ± 0,17	17,48 ± 0,44	17,41 ± 0,29
IVSd (mm)	0,94 ± 0,1	0,98 ± 0,15	0,91 ± 0,05	0,84 ± 0,03
IVSs (mm)	1,23 ± 0,11	1,31 ± 0,18	1,25 ± 0,11	1,72 ± 0,11
LVIDd (mm)	3,98 ± 0,27	4,06 ± 0,12	4,14 ± 0,20	4,10 ± 0,36
LVIDs (mm)	2,79 ± 0,41	3,01 ± 0,38	3,03 ± 0,25	2,91 ± 0,39
LVPWd (mm)	0,96 ± 0,08	1,15 ± 0,3	0,93 ± 0,22	1,01 ± 0,17
LVPWs (mm)	1,24 ± 0,12	1,48 ± 0,42	1,21 ± 0,19	1,29 ± 0,21
EF (%)	57,52 ± 8,88	50,91 ± 12,27	52,61 ± 8,29	56,30 ± 7,09
FS (%)	30,10 ± 6,07	26,08 ± 7,88	26,92 ± 5,35	29,21 ± 4,47
Heart rate	429 ± 32	416 ± 29	376 ± 19	368 ± 50

BW, body weight; HW, heart weight; TL, tibia length; IVSd, interventricular septal thickness at end-diastole; IVSs, interventricular septal thickness at end-systole; LVIDd, left ventricular internal dimension at end-diastole; LVIDs, left ventricular internal dimension at end-systole; LVPWd, left ventricular posterior wall thickness at end-diastole; LVPWs, left ventricular posterior wall thickness at end-systole; EF, ejection fraction; FS, fractional shortening; Data are expressed as means ± STDEV. Data were analyzed by ordinary one-way ANOVA with Sidak's multiple comparison test.

Supplementary Table 4. Morphometric and echocardiographic characteristic of Zeb2 WT and Zeb2 cTg mice subjected to MI for 14 days.

	Zeb2 WT	Zeb2 cTg
Surgery n	sham 6	sham 6
BW (g)	30,2 ± 2,68	30,34 ± 2,89
HW (g)	0,14 ± 0,01	0,15 ± 0,03
TL (mm)	17,47 ± 0,38	17,16 ± 0,42
IVSd (mm)	0,77 ± 0,13	0,81 ± 0,09
IVSs (mm)	1,13 ± 0,14	1,22 ± 0,14
LVIDd (mm)	3,79 ± 0,15	3,99 ± 0,35
LVIDs (mm)	2,78 ± 0,17	2,77 ± 0,46
LVPWd (mm)	0,94 ± 0,18	0,79 ± 0,08
LVPWs (mm)	1,17 ± 0,2	1,11 ± 0,17
EF (%)	52,72 ± 6,03	58,33 ± 11,82
FS (%)	26,68 ± 3,85	30,88 ± 8,03
Heart rate	403 ± 31	342 ± 73
	Zeb2 WT	Zeb2 cTg
Surgery n	MI 11	MI 11
BW (g)	29,89 ± 2,82	30,48 ± 1,61
HW (g)	0,18 ± 0,03	0,16 ± 0,01
TL (mm)	17,26 ± 0,55	17,28 ± 0,44
IVSd (mm)	0,67 ± 0,14	0,76 ± 0,13
IVSs (mm)	0,71 ± 0,14 \$\$\$\$ p<0.0001	0,94 ± 0,25 # p=0.0163
LVIDd (mm)	5,46 ± 0,83 \$\$\$ p=0.0002	4,75 ± 0,65 # p=0.0389
LVIDs (mm)	5,01 ± 0,91 \$\$\$\$ p<0.0001	3,86 ± 0,97 ## p=0.0093
LVPWd (mm)	0,81 ± 0,16	0,75 ± 0,1
LVPWs (mm)	0,95 ± 0,25	1,02 ± 0,15
EF (%)	18,36 ± 8,64 \$\$\$ p<0.0001	39,22 ± 19,11 ## p=0.0036
FS (%)	8,46 ± 4,14 \$\$\$\$ p<0.0001	19,89 ± 11,32 ## p=0.0051
Heart rate	404 ± 30	376 ± 60

sham, sham-operated control group; MI, myocardial infarction; BW, body weight; HW, heart weight; TL, tibia length; IVSd, interventricular septal thickness at end-diastole; IVSs, interventricular septal thickness at end-systole; LVIDd, left ventricular internal dimension at end-diastole; LVIDs, left ventricular internal dimension at end-systole; LVPWd, left ventricular posterior wall thickness at end-diastole; LVPWs, left ventricular posterior wall thickness at end-systole; EF, ejection fraction; FS, fractional shortening; Data are expressed as means ± STDEV. Comparison of two groups was performed with the unpaired, two-tailed Student's t-test between Zeb2 WT post-MI vs Zeb2 WT post-sham (indicated by dollar sign, \$\$\$p<0.001, \$\$\$\$p<0.0001) and Zeb2 cTg post-MI vs Zeb2 WT post-MI (indicated by pound sign, #p<0.05, ##p<0.01).

Supplementary Table 5. Morphometric and echocardiographic characteristic of sham or MI subjected mice treated with AAV9-control and AAV9-Zeb2 for 14 days.

	AAV9-control	AAV9-Zeb2
Surgery	sham	sham
n	6	6
BW (g)	26,66 ± 2,77	25,75 ± 1,29
HW (g)	0,12 ± 0,01	0,13 ± 0,01
TL (mm)	16,80 ± 0,37	16,81 ± 0,19
IVSd (mm)	0,78 ± 0,09	0,75 ± 0,08
IVSs (mm)	1,09 ± 0,11	1,09 ± 0,11
LVIDd (mm)	3,86 ± 0,19	3,76 ± 0,19
LVIDs (mm)	2,93 ± 0,38	2,85 ± 0,28
LVPWd (mm)	0,79 ± 0,08	0,83 ± 0,08
LVPWs (mm)	0,95 ± 0,09	1,02 ± 0,12
EF (%)	48,56 ± 10,69	48,79 ± 9,32
FS (%)	24,36 ± 6,42	24,36 ± 5,44
Heart rate	398 ± 30	416 ± 20
	AAV9-control	AAV9-Zeb2
Surgery	MI	MI
n	10	10
BW (g)	27,96 ± 1,44	25,87 ± 2,41
HW (g)	0,16 ± 0,02	0,16 ± 0,03
TL (mm)	16,93 ± 0,44	16,76 ± 0,30
IVSd (mm)	0,64 ± 0,07 \$\$ p=0.0041	0,83 ± 0,13 ### p=0.0009
IVSs (mm)	0,68 ± 0,11 \$\$\$\$ p<0.0001	0,99 ± 0,19 ### p=0.0003
LVIDd (mm)	5,26 ± 0,78 \$\$\$ p=0.0007	4,51 ± 0,58 # p=0.0271
LVIDs (mm)	4,69 ± 0,88 \$\$\$ p=0.0003	3,67 ± 0,52 ## p=0.0066
LVPWd (mm)	0,75 ± 0,12	0,86 ± 0,08 # p=0.0302
LVPWs (mm)	0,89 ± 0,15	1,08 ± 0,11## p=0.0061
EF (%)	23,97 ± 9,76 \$\$\$ p=0.0002	38,95 ± 8,43 ## p=0.0019
FS (%)	11,21 ± 4,69 \$\$\$ p=0.0002	18,93 ± 4,68 ## p=0.0018
Heart rate	403 ± 34	401 ± 66

sham, sham-operated control group; MI, myocardial infarction; BW, body weight; HW, heart weight; TL, tibia lenght; IVSd, interventricular septal thickness at end-diastole; IVSs, interventricular septal thickness at end-systole; LVIDd, left ventricular internal dimension at end-diastole; LVIDs, left ventricular internal dimension at end-systole; LVPWd, left ventricular posterior wall thickness at end-diastole; LVPWs, left ventricular posterior wall thickness at end-systole; EF, ejection fraction; FS, fractional shortening; Data are expressed as means ± STDEV. Comparison of two groups was performed with the unpaired, two-tailed Student's t-test between AAV9-control post-MI vs AAV9-control post-sham (indicated by dollar sign, \$\$p<0.01, \$\$\$p<0.001, \$\$\$\$p<0.0001) and AAV9-Zeb2 post-MI vs AAV9-control post-MI (indicated by pound sign, #p<0.05, ##p<0.01, ###p<0.001).

Supplementary Table 6. Morphometric and echocardiographic characteristic of sham or MI subjected mice treated with AAV9-control and AAV9-Zeb2 for 28 days.

	AAV9-control	AAV9-Zeb2
Surgery	sham	sham
n	6	6
BW (g)	25,61 ± 1,83	28,06 ± 2,12
HW (g)	0,14 ± 0,02	0,13 ± 0,01
TL (mm)	16,70 ± 0,34	17,04 ± 0,44
IVSd (mm)	0,77 ± 0,09	0,77 ± 0,09
IVSs (mm)	1,03 ± 0,16	1,05 ± 0,13
LVIDd (mm)	3,91 ± 0,55	4,00 ± 0,27
LVIDs (mm)	3,20 ± 0,45	3,31 ± 0,33
LVPWd (mm)	0,75 ± 0,12	0,79 ± 0,17
LVPWs (mm)	0,87 ± 0,10	0,97 ± 0,22
EF (%)	38,09 ± 1,57	36,22 ± 10,81
FS (%)	18,07 ± 0,94	17,34 ± 6,04
Heart rate	426 ± 29	432 ± 54
	AAV9-control	AAV9-Zeb2
Surgery	MI	MI
n	10	10
BW (g)	27,43 ± 2,45	28,95 ± 2,45
HW (g)	0,16 ± 0,03	0,17 ± 0,03
TL (mm)	17,00 ± 0,28	17,29 ± 0,50
IVSd (mm)	0,71 ± 0,13	0,83 ± 0,13 # p=0.0301
IVSs (mm)	0,79 ± 0,22 \$ p=0.0310	0,96 ± 0,25
LVIDd (mm)	5,29 ± 0,89 \$\$ p=0.0034	5,28 ± 0,78
LVIDs (mm)	4,89 ± 0,99 \$\$ p=0.0012	4,64 ± 0,96
LVPWd (mm)	0,82 ± 0,09	0,84 ± 0,12
LVPWs (mm)	0,93 ± 0,12	1,04 ± 0,14 # p=0.0413
EF (%)	17,27 ± 9,05 \$\$\$ p<0.0001	26,56 ± 12,24 # p=0.0499
FS (%)	7,912 ± 4,28\$\$\$\$ p<0.0001	12,61 # 6,21 # p=0.0451
Heart rate	450 ± 59	431 ± 45

sham, sham-operated control group; MI, myocardial infarction; BW, body weight; HW, heart weight; TL, tibia lenght; IVSd, interventricular septal thickness at end-diastole; IVSs, interventricular septal thickness at end-systole; LVIDd, left ventricular internal dimension at end-diastole; LVIDs, left ventricular internal dimension at end-systole; LVPWd, left ventricular posterior wall thickness at end-diastole; LVPWs, left ventricular posterior wall thickness at end-systole; EF, ejection fraction; FS, fractional shortening; Data are expressed as means ± STDEV. Comparison of two groups was performed with the unpaired, two-tailed Student's t-test between AAV9-control post-MI vs AAV9-control post-sham (indicated by dollar sign, \$p=0.05, \$\$p<0.01, \$\$\$p<0.0001) and AAV9-Zeb2 post-MI vs AAV9-control post-MI (indicated by pound sign, #p<0.05).

Supplementary Table 7. List of primers used in this study.

Gene	Species	Purpose	Forward	Reverse
Zeb2	mouse	QPCR	gagcaggtaaccgcagaatc	aagcgttctgcagttgg
App	mouse	QPCR	gaatggaaagtgggagtcagac	accagtctggatggtactg
Basp1	mouse	QPCR	cgggagagagagagcccttg	cttcctctgcacgttgcc
Clic1	mouse	QPCR	cacagacaccaacaagatcgag	ttgcaaataatgtccagtcgg
Dynll1	mouse	QPCR	gaaggatattgcggccatatac	agtgtttggttcatgtgtcac
Ptma	mouse	QPCR	caccaaggactgaaggagaag	ctaccatgtcagccctcg
Rack1	mouse	QPCR	gaggtaactccacattcgtag	gacaatgcctgtgtgt
Spcs2	mouse	QPCR	agaaacttcgtggatgactcg	atcccaaataaagccacgatg
Tapbp	mouse	QPCR	ggccatgttgcacccaaagc	gatgaaggcgtcatctcg
Tmsb4	mouse	QPCR	aacgcaagagaaaaatccctg	aaataagaaggcaatgtcg
Tmsb10	mouse	QPCR	taaggccaagctgaagaaaaacc	gggtctggagatgtgggg
Ywhab	mouse	QPCR	ggacacgaacttcataaag	ctgctgtttcttcattctc
Pecam1	mouse	QPCR	gaacgaaaggctccat	ggggacaggctataaatcag
Vegf (all isoforms)	mouse	QPCR	tgcggatcaaaccctccaaa	ctggcttgttctgtttttgg
Sfrp2	mouse	QPCR	gaagctccaaaccataaag	ctgtctttgttccaggatg
Gpnmb	mouse	QPCR	gaatggatgaacaccgttatcc	ccacaaaatgtatgtggaaatc
Thbs1	mouse	QPCR	caaggcatgtatctctctcc	gtgcaaaggagatgtcaatg
Eln	mouse	QPCR	gttcccggtggagttatattc	ctccaaacgttcccagaagtc
Egf	mouse	QPCR	aagagtttccataacggacag	tgactccgttctgtgtctac
Epn3	mouse	QPCR	agtgcgaagaggctaaag	cactggagatgtatcccttc
Myot	mouse	QPCR	aaatgcaaagacacccttcc	tatgtgttgtaatcttggac
Mybpc2	mouse	QPCR	atcaagtgttcaagggaaag	acggtgtacacatgtgtgtc
Gata2	mouse	QPCR	tgtcttcataaccatctcgac	gtgtcaacaaggatgtgtc
Acta2	mouse	QPCR	accacccagatggagaag	agcatcatcaccacggcag
Notch1	mouse	QPCR	ccctgtctgcctcaacg	gcagacacaggctcagtc
Zeb2	rat	QPCR	ccgtggacctgtcattacc	ggatgaagaaaactgtgtgg
App	rat	QPCR	aatggaaaatgggagtcagacc	accagtctggatggtactg
Basp1	rat	QPCR	gaaggagagcgaaccccg	cttgcggcccttttc
Clic1	rat	QPCR	gagtacccatcaacgttaccc	tgttgtatctgtgtcactc
Dynll1	rat	QPCR	cacggtaaccatgtgcac	tacttccaaacgcctgt
Ptma	rat	QPCR	ggaggcagagaatgtgaagagac	cttctcaccatcaccc
Rack1	rat	QPCR	tgttagcgatgtgtcatctcc	gacaaatgtctgtgtgt
Spcs2	rat	QPCR	ccgcagttgttgtgtgataag	gagaccgaagttccacatac
Tapbp	rat	QPCR	cggccagatctgtacccttaag	gaacgggatgtgtgtc
Tmsb4	rat	QPCR	gatgcaaaagagggtgtgataag	catgcaagtctttcc
Tmsb10	rat	QPCR	taaggccaagctgaagaaaaacc	ttctggagatgtgggtgg
Ywhab	rat	QPCR	gtaacagacggggatgtgaaac	ctgctgtttcttcattctc
Col1a2	rat	QPCR	tggaaaacccttgaagactg	atccagaccgtgtgtcc
Col3a1	rat	QPCR	agctggaccaaagggtgt	gacccgtgtccaggatgc
Bcl2	rat	QPCR	gtgacacaatctgtgt	ctgagcagcgttccagaga
Vegf (all isoforms)	rat	QPCR	gccccatcaaaccatcaca	tggcttgttctatcttcttgg
Pecam1	rat	QPCR	atatacgccacccatcgaaatc	agactgagaaatgtcaacc
ZEB2	human	QPCR	gacatccagaaaaggatgtcc	gaaggcttgatgtgtgtcc
TMSB4	human	QPCR	aacgaagaaaaatccctg	aaataagaaggcaatgtcg
PTMA	human	QPCR	caccaccaaggacttaaggag	cttcgttccatgtgtc
VEGFR1	human	QPCR	gctcagctgtgtcttcac	agaccattatgtggctgt
VEGFR2	human	QPCR	caggatcgacggaaatgtcc	ctggcagatcaagagaaac
FGF2	human	QPCR	tgccaaaggctgaaatgtcc	ctccgttccatcaaaag
NOTCH1	human	QPCR	ggaggcatctaccctttc	tgttgtgtggatgttcc
MIKI67	human	QPCR	aaaaggatccatcagcaagcc	ccctacttcataatgttcc
PCNA	human	QPCR	gaacctcaccatgttccaaaatc	ctttctctgggtgtgtcc
CDK4	human	QPCR	aatgcacgttccaggatgt	gagtgtaacaaccacgggtgtaa
Cre		genotyping	gaagcaactatgtgtttacg	cactatccaggatgtgtgtcc
Zeb2 floxed allele		genotyping	(intron 6) gaactgtgttgcataatgggg	(intron 6) atcagcagccctatataacagatgtc
Zeb2 knock in		genotyping	aaagtgcgttgcgtgttat	(intron 7) aagcatgtcggtaaatgtgttgcataacc
		genotyping		(wild type) ggacggggagaaatgtgtatg (knock in) gcgaaagatgtgtgtccaa